Milan ŠEBÖK[1], Miroslav GUTTEN[1], Matej KUČERA[1], Daniel KORENČIAK[1], Tomasz N. KOŁTUNOWICZ[2]

University of Žilina, Zilina, Slovakia (1), Lublin University of Technology, Lublin, Poland (2)

Nondestructive diagnostics of electrical systems and equipments

Abstract. *This paper analyses the problem of thermal sensors, it examines the principles, functions and application for a non-contact temperature measurements. The knowledge in measurements of infrared radiance allows us to use the methods of thermovision diagnostics more effectively and to localise the disturbance which determines the quality of connection in distribution of electric energy. For technical testing of electrical systems and equipment thermography is an important diagnostic method for determining of failure of electrical systems and equipment as well as for detection of worsened condition of these systems.*

Streszczenie. *W artykule przedstawiono problematykę termicznych sensorów, zasady badań uwzgledniające bezdotykowe pomiary temperatury, ich funkcje oraz wnioski. Dotychczasowa wiedza o pomiarach w podczerwieni pozwala na efektywniejsze wykorzystanie metod termowizyjnych celem lokalizacji zakłóceń związanych z jakością połączeń odpowiadających za dystrybucję energii elektrycznej. Termografia jest nieniszczącą metodą diagnostyczną pozwalającą na badania instalacji elektrycznych i sprzętu w celu określenia uszkodzeń urządzeń i systemów elektrycznych, a także do wykrywania pogarszania się ich stanu. (**Nieniszcząca diagnostyka systemów elektrycznych i urządzeń**).*

Keywords: Thermovision, radiation, calculation, thermogram.
Słowa kluczowe: Termowizja, promieniowanie, kalkulacja, termogram.

doi:10.12915/pe.2014.03.41

1. Introduction

In measurement of electrical equipment and wires we deal with warming of contacts, switches, power cables, clamps, contacts of fuses. In electrical substation, temperature of each object is measured, focusing on the expansion joints, junctions, bends and coats drivers.

Thermovision is used to measure warming of connections and clamps in electrical machines, as well as to the measurement of electrical equipments in the internal and external electrical distributing systems. Fundamental for a non-destructive diagnostics of electrical equipments using thermovision, is the ability to record and to transform infrared radiation (heating) to the form of real thermal images of objects, for a detection of a failure (defect) [6].

Infrared radiation is generated as a result of physical processes that take place in the object of radiation; moving atoms, molecules, vibration in crystal lattice, and transition of electrons from one energy level to another. The basic source of infrared radiation is elevated temperature of the source of radiation [3].

Radiation of hot sources acts (in respect of surrounding conditions), like visible light. To display temperature fields we can use visualization techniques used in optics. The only differences are materials used for elements of visualization systems, size of values which are derived from the wavelength of radiation, and also sensitivity of sensors for recording the signal [6].

The surface of the measured object in a state of thermodynamic equilibrium emits electromagnetic radiation and the radiated power depends on the thermodynamic temperature and properties of the surface object.

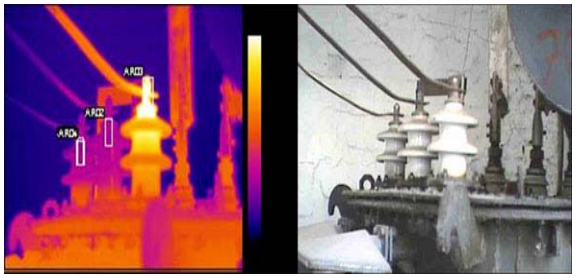

Fig.1. Termogram and real picture of transformer

For thermovision diagnostics of infrared radiation in the inside distribution of electric energy, we need to take into account many important factors affecting the accuracy of measurement. Results of the measured values of specific electric contact are often biased by measurement defects. In determining the classification of degrees to correct the defects, it is necessary to correct measured values due to disruptive effects of other objects [1].

2. Theory

Thermal Sensors are equipment, which transform input physical quantity (temperature) to electric signal. Transformed signal can be used in automatic control systems for data records elaboration and archivation [2].
Infra-radiation, which is absorbed to the active part of a sensor, increases its temperature. Temperature changes in the sensitive part of a sensor are represented by a relative slow process. In Fig.2 is a model – by construction of the thermal sensor [5].

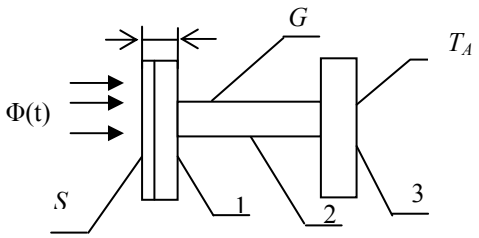

Fig.2. Model – Simple construction of thermal sensor: 1 - sensitive part of sensor with temperature T_D, active area of sensor S and thickness d, 2 - thermal bridge with thermal conductivity G, 3 - base with temperature T_A

If the sensitive part of sensor is characterised with heat capacitance C, absorbtance α and it is conducted surround area with temperature T_A, with thermal conductivity G and active sensor is radiated with radiance current $\Phi(t)$, that changes with time, then if holds:

$$\text{if } \Phi(t) = 0 \text{ then } T_D = T_A$$
$$\text{if } \Phi(t) > 0 \text{ then } T_D > T_A \quad (1)$$

The state of the thermal balance occurs when the absorbed energy is equal conductive thermal energy of the thermal bridge [5].

By the following differential equation is described:

(2) $$\alpha\Phi(t) = C\frac{d}{dt}[\Delta T(t)] + G\Delta T(t),$$

where: $\Delta T = T_D - T_A$ is temperature increase of sensitive part of sensor, when this part is heated with absorbed input radiance current $\alpha\Phi(t)$. Let the radiance input current change in time

(3) $$\Phi(t) = \Phi_0 + \Phi_m e^{j\omega t}$$

The result for the temperature increase is

(4) $$\Delta T(t) = T_0 + \Delta T_m e^{j(\omega t-\varphi)}$$

The first term is the d.c. part and the second term is the harmonic part this equation [6]. On the basis of formulations (3), (4) we can design electrical (substitute) structure of thermal sensor Fig.3.

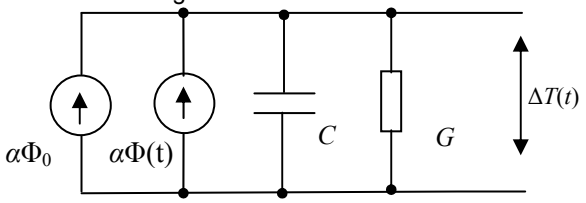

Fig.3. Electrikal structure of thermal sensor

Temperature increase ΔT is delayed against input radiance current $\Phi(t)$. For amplitude ΔT_m and shift movement period φ we write

(5) $$\Delta T_m = \frac{\alpha\Phi_m}{\sqrt{G^2 + (\omega C^2)}} \text{ and } \varphi = arctg\left(\frac{\omega C}{G}\right)$$

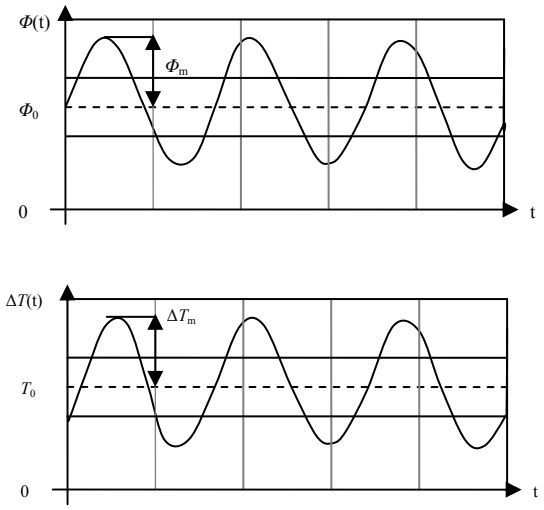

Fig.4. Input radiance current and delay of the temperaturel of thermal sensor

3. Radiation

Heating is defined by the relationship α/ε, where α is the absorption coefficient of energy and ε is the emission coefficient (emissivity) of the measured body [1].

Ratio of intensity radiation of actual body and ideal black body at the same temperature is defined by spectral coefficient of emissivity [8]:

(6) $$\varepsilon_\lambda(\lambda,T) = \frac{H_\lambda(\lambda,T)}{H_{0\lambda}(\lambda,T)}$$

It is clear that the coefficient of spectral emissivity is equal to the spectral absorption coefficient. By Kirchhoff's law the black body is an ideal emitter. Plank defines the spectrum of black body radiation [8]:

(7) $$\frac{dH(\lambda,T)}{d\lambda} = \frac{2\pi hc^2\lambda^{-5}}{e^{\frac{hc}{\lambda kT}} - 1}$$

Plank's law is a function of spectral distribution of values. Win's law clearly defines the shift of visible and invisible body radiation (when it is heated) to the side of the shorter waves. Stefan-Boltzmann's law, as an integration of Planck's law by λ, defines an integral radiant flux density of black body at the temperature T [3]:

(8) $$H_T = \int_0^\infty [dH(\lambda,T)/d\lambda]d\lambda = \sigma T^4$$

where: σ = 5,67.10^{-8} W/m^{2}K^4 – Boltzmann constant.

Flux density of blackbody radiation (Fig.5) on the range of wavelengths λ_a, λ_b is received by integrating Planck equation by λ [6].

(9) $$H_T = \int_{\lambda_a}^{\lambda_b} [dH(\lambda,T)/d\lambda]d\lambda = \sigma T^4$$

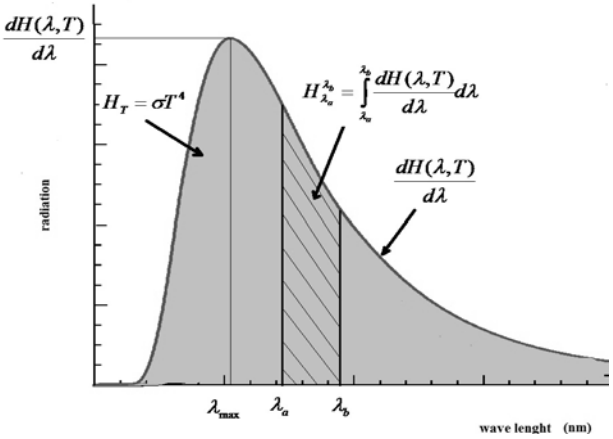

Fig.5. Flux density of black body radiation

Derivation of Planck's equation by temperature dT gives the change of spectral flux density emitted from black body as a function of temperature [6]:

(10) $$\frac{\partial(dH/d\lambda}{\partial T} = \frac{(hc/k)e^{(hc/\lambda kT)}}{\lambda T^2\left[e^{(hc/\lambda kT)} - 1\right]} \cdot \frac{dH}{d\lambda}$$

Real objects generally do not behave as black bodies. No-black bodies absorb only a part of $\alpha(\lambda)\Phi$ (incident radiation), part of the reflected radiation $\varepsilon(\lambda)\Phi$ and part $\tau(\lambda)\Phi$ is a transient radiation. If the system is in thermodynamic equilibrium, according to conservation of energy, the reflected and transient energy is equal to the energy absorbed. Emissivity $\varepsilon(\lambda)$ (coefficient of radiation), compensates absorption coefficient $\alpha(\lambda)$ then $\varepsilon(\lambda) = \alpha(\lambda)$. It follows that:

(11) $$\varepsilon(\lambda) + \rho(\lambda) + \tau(\lambda) = 1$$

The result of object temperature measurement T_0, which is registered in the spectral range of wavelengths $\Delta\lambda$

(surface density of radiant flux), is the registered radiant flux density H_{reg} [6]:

$$H_{reg} = \int_{\Delta\lambda} \rho_a(\lambda)\left[dH(\lambda,T_a)/d\lambda\right]d\lambda + \\ + \int_{\Delta\lambda} \tau_f(\lambda)\left[dH(\lambda,T_f)/d\lambda\right]d\lambda + \\ + \int_{\Delta\lambda} \varepsilon_0(\lambda)\left[dH(\lambda,T_0)d\lambda\right]d\lambda \tag{12}$$

When an object is transparent $\tau(\lambda) = 0$ and if T_0 is much larger than T_a, the first part of the equation is very small. In this case the task is easier and it is essential to know $\varepsilon_0(\lambda)$. Difficulties arise when the body is surrounded by other objects, which have high temperature and these temperatures are higher than the examined object. In this case, its own radiation depends on the T_0 and ε_0 affected by reflected radiation error caused by parasitic (surrounding) objects with a temperature T_e and emissivity ε_e.

For measurements of this type it is necessary to know ε_0 and T_0 parameters and the number of equations, which are equal to number of unknown parameters. Radiation of measured object is formed by the sum of two parts; its own H_1 radiation and parasitic H_2 radiation in the infrared spectral range:

$$H_1 = S\int_{\Delta\lambda_1} \rho_e(\lambda)\varepsilon_e(\lambda)\left[dH(\lambda,T_e)/d\lambda\right]d\lambda + \\ + \int_{\Delta\lambda_1} \varepsilon_0(\lambda)\left[dH(\lambda,T_0)/d\lambda\right]d\lambda \tag{13}$$

$$H_2 = \int_{\Delta\lambda_1} \varepsilon_e(\lambda)\left[dH(\lambda,T_e)/d\lambda\right]d\lambda$$

where: S - geometric parameter which depends on the distance of two objects and on their surfaces.

4. Experimental

In measurement of electrical equipment and wires we deal with warming of contacts, switches, power cables, clamps, contacts of fuses. In electrical substation temperature of each object is measured, focusing on the expansion joints, junctions, bends and coats drivers. A circuit containing conductor was set up in the laboratory.

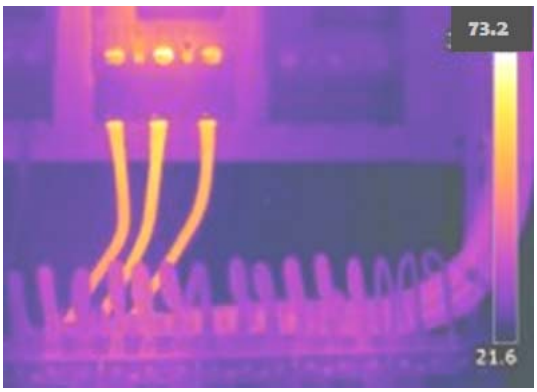

Fig.6. Thermogram of breaker

The conductor was divided into three parts connected to the staples. The three phase breaker was derived from harmonic current. The thermogram of the circuit is on the Fig. 6.

The measured circuit was load by the current from 5% to 100% of the conductor's nominal current load [7].

The measurements were taken under the following conditions:

- clean and well closed terminal,
- loose terminal (terminals were loose and conductors were connected only through their asymmetric position),
- loose terminal and staple and conductor connection was tained with oil and sand.

Measured results are graphicaly illustrated on the Fig. 7. Staple connected to the conductor cant be warmer than free conductor, if it is not damaged.

On the picture we can see the negative area of the staple temperature increase compared with the closed conductor. The result of the smaller staple temperature is caused by the bigger load.

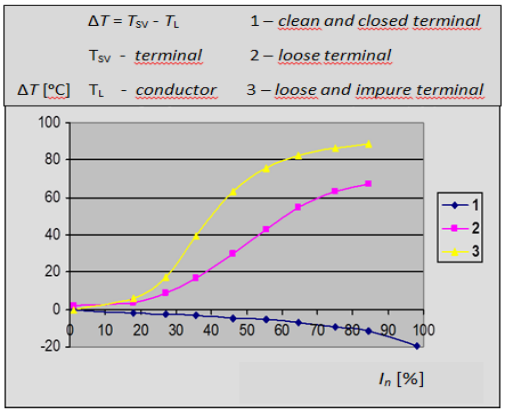

Fig.7. Relation of the staple temperature increase and current load

The final data of the staples temperature increase compared to the conductors are illustrated on the Fig.7 which means $\Delta T = T_{SV} - T_{L,}$ (T_{SV} is the terminal temperature and T_L is conductor temperature) and they were obtained by the temperature measurements of the electric joints and conductors.

Fig.8 Termogram high voltage breakers

On the Fig. 8 we can see the thermogram of measured object at a temperature T_1 and emissivity ε_1 which we want to know (radiant 1. and 3. phase with temperature T_1 and T_3) and from the other side we can see parasitic object with temperature T_e, which is larger than T_1 and T_3 (radiant phase 2).

Emissivity ε_e of parasitic object is high and the distance from measured object *d* is small. The temperature value T_e and emissivity ε_e is unknown. The thermal camera distinguishes this different temperature of objects, i.e. temperature, which would have absolutely black body in this spectral range.

The result of calculated equation is the temperature of 2. phase (parasite object) T_e = 352.65 K. Value of calculated

temperature T_e is near to measured temperature T_e = 352.65 K.

The size of radiation flux density of parasite object BR2 (ε_e = 0.96 and temperature T_e = 352.65 K) is:

$$H_e = \varepsilon_e \int_{\Delta\lambda_1} [dH(\lambda, T_e)/d\lambda] d\lambda \tag{14}$$

Then the radiant flux density of the 1 and 3 phase measured object is:

$$H = \varepsilon_0 \int_{\Delta\lambda} [dH(\lambda, T_0)/d\lambda] d\lambda + \quad radiation$$
$$(1-\varepsilon_e)\varepsilon_e S \int_{\Delta\lambda} [dH(\lambda, T_e)/d\lambda] d\lambda \quad reflection \tag{15}$$

If S = 1 then we have result calculated temperature of measured object (1. phase of breaker) with T_1 = 293.15 K, and (3. phase of breaker) with T_3 = 294.45 K

For Measured data:
F1: T_1 = 327.45, K = 54.30ºC, ε_1= 0.96
F2: T_e = 352.65, K = 79.50ºC, ε_e= 0.96
F3: T_3 = 338.19, K = 65.04ºC, ε_3= 0.96

Following values were calculated:
F1: T_1 = 303.25, K = 30.10ºC, ε_1 = 0.85
F2: T_e = 348.45, K = 75.30ºC, ε_e = 0.92
F3: T_3 = 306.19, K = 38.04ºC, ε_3 = 0.89

5. Conclusion

Comparing the results of calculated and measured values; we see that real measured temperature values are influenced by parasite object. The differences between the calculated and measured values are illustrated on the graph (Figs. 9, 10, 11).

On the graph we see measured and calculated temperature differences of breaker phase F3 at the current load. Measured temperature of breaker (phase F1 and F3) is higher than calculated because close parasite object breaker F2 influences its temperature. As we can see on the graph (Fig. 6) temperature differences depend on the value of current load (*In*).

Experimental measurements and mathematical calculations show the advantage of thermovision application on the illustrated diagnostics of the conductors and staples temperature increase. It is necessary to consider the parasitic effects of warming measured electrical systems.

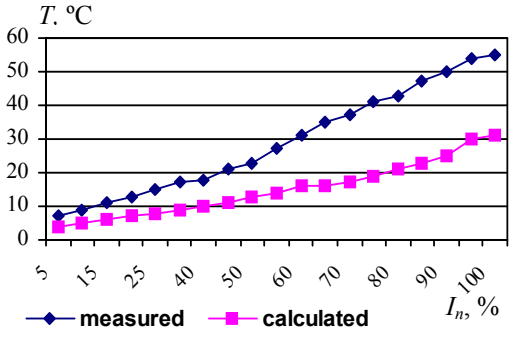

Fig.9. Measured and calculated data (phase F1)

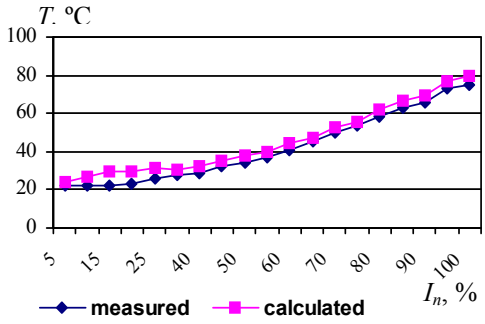

Fig.10. Measured and calculated data (phase F2)

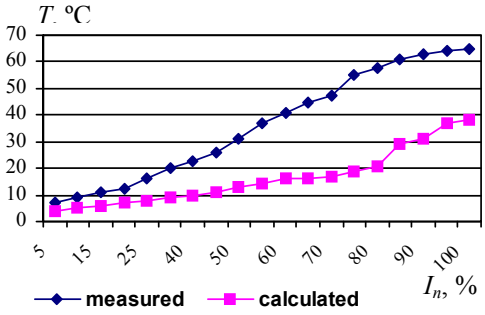

Fig.11. Measured an calculated data (phase F3)

This work was supported by the Grant Agency VEGA from the Ministry of Education of Slovak Republic under contract 1/0624/13. Dr. T.N. Koltunowicz is a participant of the project: "Qualifications for the labour market – employer friendly university", cofinanced by European Union from European Social Fund.

REFERENCES

[1] Benko I., Determination of the Infrared surface Emisivity, Budapest, 1990
[2] Pender C.W., Roux J.A., Microcomputer System for controling and Infrared Scaning Camera. Microcomputer in optical System, USA,1999
[3] Toth, D., Infrared System Helps with Energy Efficiency, USA, 1995
[4] Klabacka E., Surface modifications for Thermovision Measurement, ČVUT, Prague 2001
[5] Lysenko V., Detectors for noncontact temperature measurement, Prague 2005
[6] Šebök M., Gutten M., Kučera M., Diagnostics of electric equipments by means of thermovision, *Przeglad Elektrotechnicny*, 87 (2011), n. 10, 313-317
[7] Kúdelčík J., Bury P., Drga J., Kopčanský P., Závišová V., Timko M., Structure of transformer oil-based magnetic fluids studied using, *Journal of Magnetism and Magnetic Materials*,326 (2013), n.1, 75-80
[8] Šimko M., Chupáč M., The theoretical synthesis and design of symmetrical delay line with surface acoustic wave for oscillators with single-mode regime of oscillation, *Przeglad Elektrotechniczny*, 88 (2012), n.12A, 347-350

Authors:
Dr. Milan Šebök, Ph.D. (Eng), Prof. dr. hab. Miroslav Gutten, Ph.D. (Eng), Dr. Matej Kučera, Ph.D. (Eng), Dr. Daniel Korenčiak, Ph.D. (Eng), Department of Measurement and Application Electrical Engineering, Faculty of Electrical Engineering, University of Žilina, 1, Univerzitná Str, 01026 Žilina, E-mail: milan.sebok@fel.uniza.sk, gutten@fel.uniza.sk;
Dr. Tomasz N. Kołtunowicz, Ph.D. (Eng), Faculty of Electrical Engineering and Computer Science, Department of Electrical Apparatus and High Voltages Technology, Lublin University of Technology, 38a, Nadbystrzycka Str., 20-618 Lublin, Poland, E-mail: t.koltunowicz@pollub.pl.